The Canadian Mineralogist
Vol. 35, pp. 923-935 (1997)

VERY LOW-GRADE CHLORITE WITH ANOMALOUS CHEMISTRY AND OPTICAL PROPERTIES FROM THE MALAGUIDE COMPLEX, BETIC CORDILLERAS, SPAIN

MARIA DOLORES RUIZ CRUZ

Departamento de Química Inorgánica, Cristalografía y Mineralogía, Facultad de Ciencias,
Universidad de Málaga, E-29071 Málaga, Spain

ABSTRACT

Two generations of chlorite, in very low-grade metaclastites from the Maláguide Complex (Betic Cordilleras, southern Spain) ascribed to Variscan and to Alpine metamorphic events, have been characterized by microscopy, chemical analysis, XRD, IR and DTA–TG. All of these chlorites show abnormal optical properties and low $^{IV}Al/^{VI}Al$ ratios if all iron is considered as ferrous iron. Nevertheless, results of electron-microprobe analyses show a slight excess of H_2O, and a chemical determination of ferrous iron indicates Fe^{3+}/Fe^{2+} ratios in the order of 0.25. On the basis of the octahedral occupancy, these chlorites may be considered as a transition from tri- to di,trioctahedral minerals. Although these chlorites differ widely from Al-rich di, trioctahedral chlorites (sudoite or cookeite) in Al content, their di,trioctahedral nature is also supported by the IR spectra and the thermal behavior. Optical properties also agree and correlate with an appreciable Fe^{3+} content. The chlorites evolve during the Variscan metamorphism by showing a slight increase in Fe content. Prograde Alpine metamorphism produced a simultaneous increase in tetrahedral Al and Fe/(Fe + Mg).

Keywords: chlorite, Alpine orogeny, Betic Cordilleras, Maláguide Complex, very low-grade metamorphism, Variscan orogeny, Spain.

SOMMAIRE

Deux générations de chlorite des roches métaclastitiques du complexe de Maláguide, dans les Cordillères bétiques, du sud de l'Espagne, et attribuées aux événements métamorphiques varisque et alpin, respectivement, ont été caractérisées par microscopie, analyse chimique, diffraction X, spectroscopie infra-rouge, et analyse thermique différentielle et thermogravimétrique. Tous ces échantillons de chlorite font preuve de propriétés optiques anormales et d'un faible rapport $^{IV}Al/^{VI}Al$ si tout le fer est considéré à l'état ferreux. Toutefois, les résultats d'analyses à la microsonde électronique démontrent un léger excédent de H_2O, et une détermination chimique de la proportion de fer ferreux indique un rapport Fe^{3+}/Fe^{2+} d'environ 0.25. A la lumière de l'occupation des sites octaédriques, on peut considérer ces échantillons de chlorite comme exemples de la transition de variétés trioctaédrique à di,trioctaédrique. Quoique ces exemples soient très différents des chlorites di,trioctaédriques alumineuses (sudoïte ou cookeïte) dans leur teneur en Al, leur nature di,trioctaédrique est concordante avec leurs spectres infra-rouges et leur comportement thermique. Les propriétés optiques concordent avec cette hypothèse, et montrent une corrélation avec une teneur en Fe^{3+}. L'évolution des compositions de chlorite au cours du métamorphisme varisque a impliqué une légère augmentation en teneur en Fe. La progression du métamorphisme alpin a produit une augmentation simultanée en ^{IV}Al et du rapport Fe/(Fe + Mg).

(Traduit par la Rédaction)

Mots-clés: chlorite, orogenèse alpine, Cordillères bétiques, complexe de Maláguide, métamorphisme de très faible intensité, orogenèse varisque, Espagne.

INTRODUCTION

Chlorite is an important mineral in low- and very low-grade metamafic rocks, where it usually occurs as vein or vesicle fillings and as a replacement of glassy matrix or primary minerals. In very low-grade metaclastites, chlorite usually appears as a result of alteration of detrital biotite, in cases accompanied by illite, kaolinite, a smectite-group mineral or a mixed-layer mineral, which also constitute common products of alteration (White *et al.* 1985, Morad & Aldahan 1986, Beaufort 1987, Frey 1987, Jian & Peacor 1994). In most cases, low-grade metamorphic chlorite exhibits anomalous optical properties (Albee 1962), and some deviation from the ideal formula (Laird 1988, Shau *et al.* 1990).

The molar ratio Fe/(Fe + Mg) has been correlated with indices of refraction (Hey 1954, Albee 1962, Saggerson & Turner 1982), and the transition between chlorites with positive and negative optic sign has been located. Nevertheless, Albee (1962) pointed out that in some cases, chlorite from mafic meta-igneous rocks exhibits large deviations from the established trend. Such chlorite has a index lower than predicted on the basis of its Fe/(Fe + Mg) value, and it shows a negative rather than a positive optic sign. It also has more octahedrally coordinated Al (^{VI}Al) than tetrahedrally coordinated Al (^{IV}Al). Similar results have been shown in chlorite from low-grade metavolcanic rocks by Craw & Jamieson (1984) and Shau *et al.* (1990), among others.

The anomalous optic sign has been variously related to the presence of H vacancies (Albee 1962), metastable stacking sequences of polytypes of chlorite (Craw & Jamieson 1984) or mixed-layering of smectite- or vermiculite-like layers (Shau *et al.* 1990). These hypotheses will be tested with well-characterized "anomalous" chlorite from the Maláguide Complex, where this mineral replaces biotite grains, is intergrown with muscovite, and fills quartz-rich veins and segregations. This study has been carried out in order to obtain optical and chemical characterization of these different types of chlorite, and to define the chemical trend through the Paleozoic sequence. These new data establish the metamorphic conditions in which the chlorite populations have developed, either during the Variscan or the Alpine metamorphic events.

GEOLOGICAL SETTING

The Internal Zones of the Betic Cordilleras, southern Spain, include three main structural complexes (Fig. 1): Nevado-Filábride, Alpujárride and Maláguide, each with different metamorphic features. The Alpine episode of metamorphism is characterized in the Nevado-Filábride Complex by low to medium gradients. Pressures were in the order of 10–20 kbar, and temperatures, about 550°C (Díaz de Federico *et al.* 1990). The Alpujárride Complex shows important regional variations, the estimated metamorphic conditions ranging from 300–350°C at 8 kbar to about 700°C at 10 kbar (Fontboté & Vera 1984). In the Maláguide Complex, Ruiz Cruz & Andreo (1996) pointed out a clear discontinuity in the P–T conditions of the very low-grade metamorphism between Carboniferous and Permo-Triassic rocks, indicating that a Variscan episode of metamorphism affected the Paleozoic rocks prior to the Alpine metamorphic event.

The Paleozoic sequence of the Maláguide Complex (Fig. 1) comprises three members (Mäkel 1985): a) the phyllite member, b) the "calizas alabeadas" member, and c) the graywacke–shale member. The basal part of the Paleozoic is formed by varicolored phyllitic rocks. Reported fossils indicate a Silurian age (García López *et al.* 1996). The overlying sequence comprises limestone with intercalated shale and graywacke. The limestone yields conodonts of Devonian age. The bulk of the Paleozoic Unit is made up of rocks of the graywacke–shale member, consisting of a rhythmic alternation of graywacke, shale and siltstone. Fossils point to a latest Devonian to Carboniferous age.

SAMPLES AND METHODS

From a previous study of 80 samples taken in a prograde sequence of graywacke, shale and phyllite near Málaga, twelve samples were selected for the characterization of chlorite, on the basis of the following criteria. (i) The selected samples cover the various rock-types and are uniformly distributed along the Paleozoic sequence (Fig. 1). (ii) Samples with high contents of kaolinite-type minerals and those with mixed-layer minerals showing reflections at 14 and 7 Å were excluded. In this manner, the samples selected comprise graywacke, shale and phyllite, in which the main constituents are quartz, mica and chlorite, and lesser amounts of albite, carbonates, kaolinite-type minerals, mixed-layer mica–chlorite and Fe-oxides, together with vein fillings and segregations showing the quartz – chlorite – (calcite) association (Table 1).

Scanning electron microscopy (SEM) of both polished surfaces (for semiquantitative chemical analysis) and fractured surfaces of critically dried samples was undertaken in both secondary and back-scattered modes, with a JEOL JSM–840 scanning electron microscope. Areas selected from thin sections were separated, ion-thinned and carbon-coated, and examined by analytical-transmission electron microscopy (ATEM) using a 200 kV Philips CM–20 scanning-transmission electron microscope. X-ray diffraction (XRD) was used to characterize the chlorite, hand-picked from the quartz-rich veins, and to determine the mineralogy of the whole rocks and of two size-fractions (2–20 μm and <2 μm) separated by sedimentation. XRD was carried out with a Siemens D–501 diffractometer, with Cu$K\alpha$ radiation and graphite monochromator, operated at 35 mA and 40 kV. The accurate selection of samples was based on XRD patterns obtained from oriented mounts that had been air-dried, solvated with ethylene glycol and dimethylsulfoxide, and heated at 500 and 700°C.

Most of the chemical analyses of chlorite were done by electron microprobe (EMPA), using a CAMECA SX–50 instrument, under conditions similar to those recommended for clay minerals (Velde 1984). Fine-grained chlorite was characterized by analytical electron microscopy (ATEM). All chlorite compositions were recalculated on the basis of 14 oxygen equivalents (28 negative charges). At first, all Fe was assumed to be Fe^{2+}. The proportion of ferrous iron was determined chemically only for chlorite from veins and segregations, for which a sufficient amount of chlorite was available for wet-chemical analysis. Samples were decomposed with hydrofluoric acid, and the determination was carried out by titration with vanadate (Bain & Smith 1992).

Infrared spectra (IR) were recorded at room temperature over the range 4000–200 cm^{-1} on a Perkin–Elmer spectrophotometer, using KBr discs containing 2 wt.% of sample. Differential thermal analysis (DTA) and thermogravimetry (TG) were carried out on a Rigaku–Thermoflex Tas 100 with samples of 35–40 mg, heated at 10°C/min.

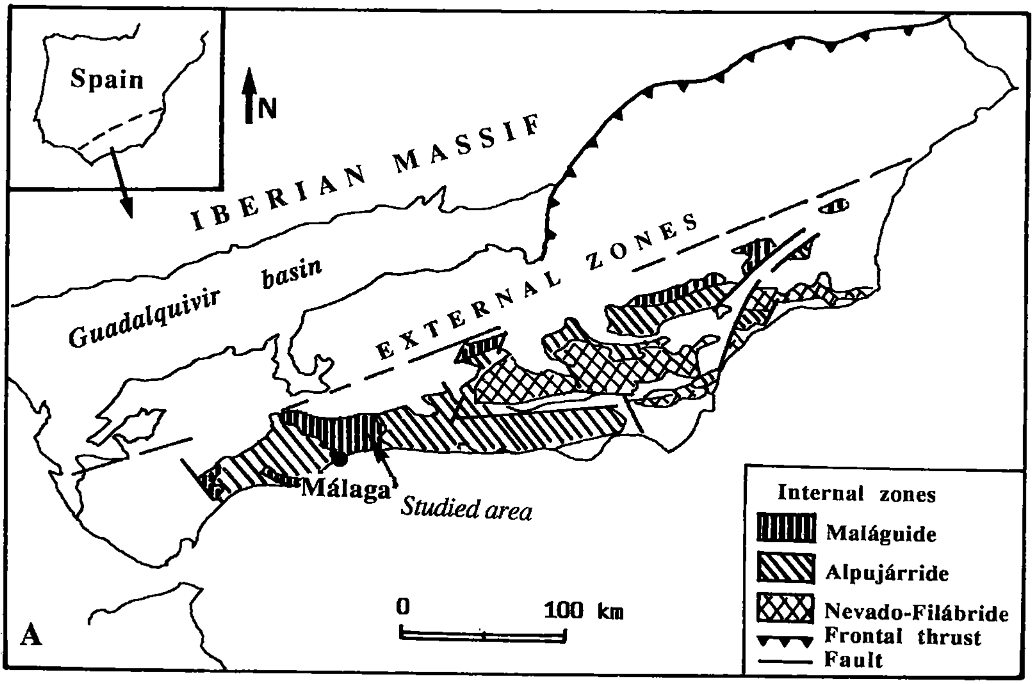

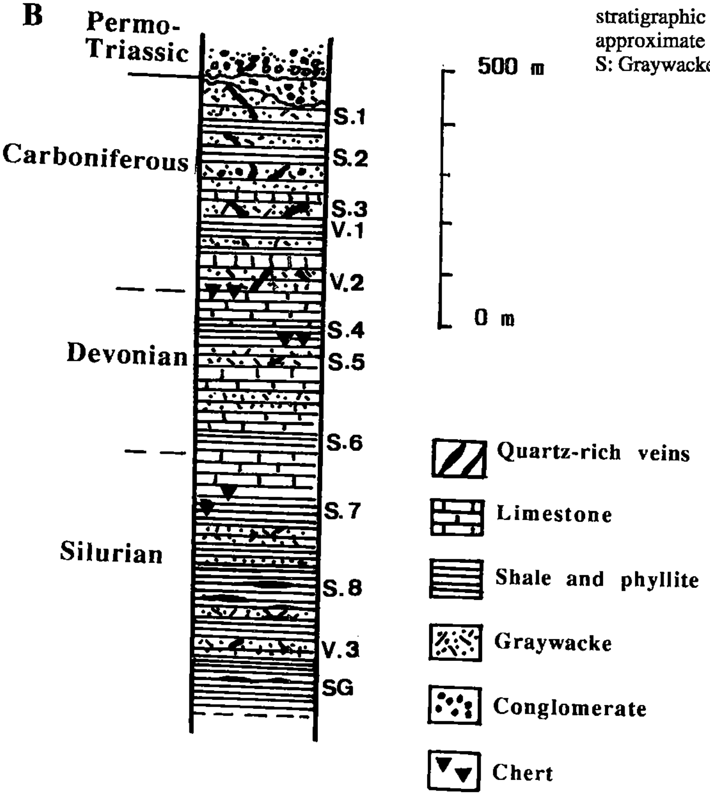

FIG. 1. A. Geological setting of the Internal zones of the Betic Cordilleras and position of the zone studied. B. Schematic stratigraphic sequence of the Maláguide Paleozoic and approximate position of the samples cited in the text S: Graywacke, shale or phyllite. V: Vein. SG: Segregation.

TABLE 1. MINERALOGICAL COMPOSITION OF SELECTED SAMPLES

		Whole rocks					<2 μm size-fraction				
Sample	Lithology	Qtz	Ab	Cal	Dol	Ph	Kln	Ms	Chl	ML	IC
1	Graywacke	42	24	Tr	–	34	–	57	43	–	0.39
2	Shale	19	10	–	–	71	–	74	26	–	0.32
3	Graywacke	42	–	–	12	46	17	59	24	–	0.27
4	Shale	36	8	8	–	48	–	65	25	10	0.26
5	Graywacke	27	21	7	–	45	–	60	40	–	0.21
6	Shale	34	16	–	–	50	–	55	45	–	0.22
7	Phyllite	72	Tr	–	–	28	–	90	10	–	0.29
8	Phyllite	71	–	–	–	29	–	85	15	–	0.20
9	Vein 1	85	–	–	–	15					
10	Vein 2	60	–	10	–	30					
11	Vein 3	90	–	–	–	10					
12	Segregation	50	–	5	–	45					

Abbreviations: Qtz: Quartz; Ab: Albite; Cal: Calcite; Dol: Dolomite; Ph: Phyllosilicates; Kln: Kaolinite-type mineral; Ms: Muscovite; Chl: Chlorite; ML: Mixed-layer minerals; IC: Illite (Ms) crystallinity.

RESULTS

The previously published results of analysis of 80 samples from the several members of the Paleozoic sequence enabled me (Ruiz Cruz 1995, 1996) to establish the main assemblages of minerals (Table 2), which are dependent on both stratigraphic position and rock type. Chlorite is widely distributed in the Paleozoic sequence, although it is better developed in: a) shale from member 3 (Carboniferous), b) graywacke from member 2 (Devonian), c) phyllite from member 1 (Silurian), d) quartz-rich veins, particularly abundant in member 3, and e) segregations, frequent in member 1.

Some types of chlorite, showing variable interference-colors, have been identified in the samples studied. (i) Grains of brown chlorite of variable size (so-called "oxidized chlorite"), and (ii) colorless to blue chlorite, developed from detrital biotite, to be referred to as "chlorite after biotite" are common in Carboniferous and Devonian graywackes, and are clearly detrital in origin. They are oriented parallel to bedding and appear deformed (Fig. 2A). (iii) Stacks of chlorite + mica consist of parallel to subparallel rectangular packets of chlorite and muscovite, which are subparallel to bedding and display deformation features that imply an origin preceding the main phase of deformation (Fig. 2B). (iv) Scarce interstitial chlorite appears as small parallel or radiating aggregates in graywackes, without relation to the bedding, commonly replacing quartz grains or other mineral phases. (v) Colorless to green vermicular chlorite fills quartz and calcite-rich veins up to 25 cm in thickness, common in the Carboniferous member. (vi) Radiating arrays appear along the walls of quartz-rich thin veins (Fig. 2C). This type of vein, which appears to be structurally related to Alpine deformation, occurs commonly in coarse-grained beds throughout the Paleozoic sequence. (vii) Chlorite aggregates are associated with quartz segregations parallel to the schistosity, in early Paleozoic phyllite.

The various types of chlorite differ in their optical properties. Refringence and birefringence increase in the sequence: chlorite from Alpine-type veins → chlorite from chlorite–mica stacks → chlorite from segregations → chlorite after biotite → oxidized chlorite. In most cases, the chlorite shows a positive elongation, indicating that the optic sign is negative. Nevertheless, chlorite from veins commonly show a variable sign of elongation along single crystals (Fig. 2C).

TABLE 2. MAIN MINERAL ASSEMBLAGES IN PALEOZOIC SAMPLES FROM THE MALAGUIDE COMPLEX

	Main lithotypes	Assemblage
Member 3	Graywacke	Quartz-mica-dickite/nacrite-tosudite-dolomite
	Shale	Quartz-albite-mica-chlorite-calcite
Member 2	Graywacke	Quartz-albite-mica-chlorite-calcite
	Shale	Quartz-albite-mica-chlorite-Ms/Chl mixed-layer-calcite
Member 1	Phyllite	Quartz-albite-mica-chlorite-corrensite-calcite
	Schist	Quartz-albite-mica-(chlorite)

Minor amounts of Fe- and Ti-oxides, apatite and zeolites are common constituents of these rocks. Ms: Muscovite. Chl: Chlorite.

SEM examination of chlorite from veins shows either vermicular aggregates of euhedral crystals of chlorite, intimately intergrown with quartz or calcite (Fig. 3A), in thick veins, or aggregates of large crystals of chlorite, slightly curved with occasional development of nacrite, in Alpine-related veins (Fig. 3B).

TEM images of chlorite samples vary according to the type of chlorite examined. Chlorite–mica stacks show

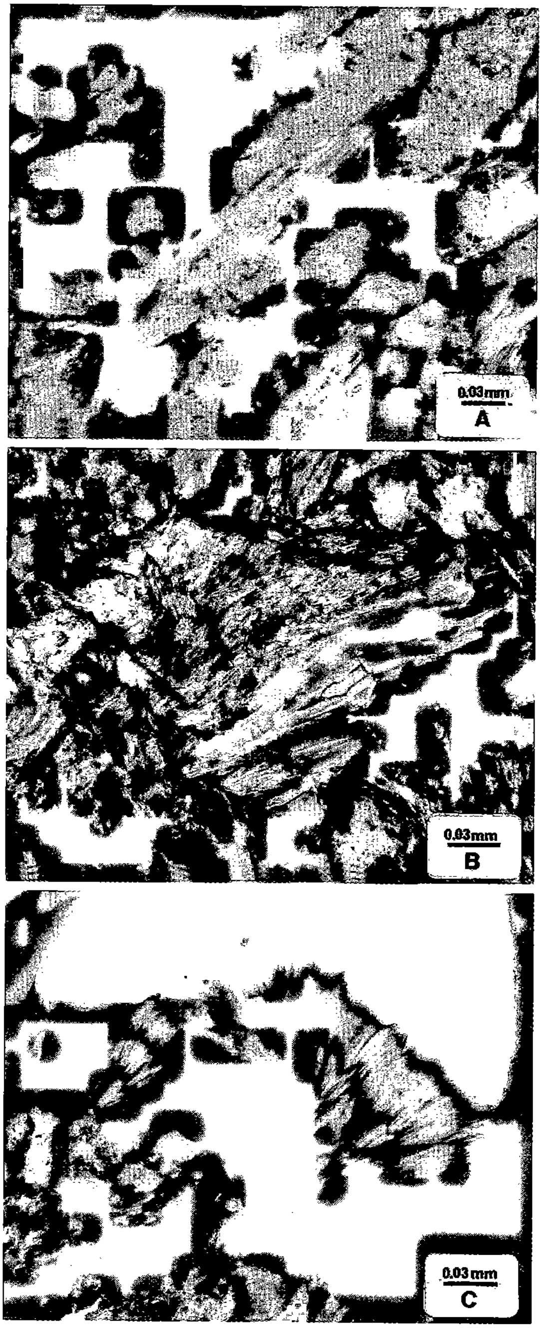

FIG. 2. Photomicrographs showing different types of chlorite. A. Oxidized chlorite parallel to bedding. Sample 1. B. Chlorite–mica stacks. Sample 5. C. Quartz-rich vein from the upper Carboniferous, showing radiating crystals of chlorite with a double inversion of the sign of elongation. Vein 1.

chlorite packets in the order of 500–1000 Å in thickness, interleaved with muscovite packets, but mixed-layer units with successive chlorite and muscovite layers are not observed (Fig. 4A). The SAED patterns of the stacks show the $00l$ reflections of both chlorite and muscovite. In comparison, chlorite from veins is monomineralic, consisting of stacks of many packets of chlorite layers, each packet several hundred Å in thickness. The $00l$ lattice-fringe images (Fig. 4B) display uniform 14 Å periodicity through the packets. The SAED patterns show in this case intense basal reflections and reveal a two-layer polytype.

Chemical data

The results of electron-microprobe analyses of chlorite from graywacke and vein, characterized optically, are listed in Table 3. Overall, the analyzed samples show little variation in Si and Al contents, and a large variation in the ratio Fe/(Fe + Mg). Thus, in the Si – Al – (Fe + Mg) diagram (Fig. 5A), the chlorite samples occupy a limited field that overlaps to a great extent the field of metamorphic chlorite (Velde 1985). In the Al – Fe – Mg diagram, the chlorite samples occupy a larger field, and some zones can be drawn (Fig. 5B). Chlorite from Alpine-type veins shows the greater compositional spread, related in part to the depth of the samples. Except for some chlorite grains in zone c, the data plot within the compositional band defined by Velde (1985) for metamorphic chlorite.

All the analyzed samples of chlorite show greater amounts of ^{VI}Al than ^{IV}Al, with variations (δAl = ^{VI}Al – ^{IV}Al) ranging from 0.06 to 0.62. Nevertheless, the total Ca + Na + K per formula is in all cases less than 0.1. The ^{IV}Al content shows the largest spread in chlorite samples from veins: from 0.88–1.17 atoms per formula unit (*apfu*) in late Paleozoic veins to 1.29–1.34 *apfu* in early Paleozoic veins. The remaining chlorite samples have ^{IV}Al contents ranging from 0.99 to 1.32 *apfu*. Mn content is low, and Ti content is only significant in oxidized chlorite from sample 5.

Fine-grained chlorite from shale, phyllite, vein and segregation, whose small crystal-size does not permit accurate analysis by electron microprobe, was characterized by ATEM (Table 4). Compositions thus obtained are similar to those determined by EMPA for the coarse-grained rocks.

Ferrous iron determination in chlorite from vein 2 and segregations (Table 5) indicates that these chlorites have a Fe^{3+}/Fe^{2+} ratio in the order of 0.25. However, from these analytical results the structural formula of chlorite cannot be deduced because of the presence of quartz, intimately intergrown with chlorite.

X-ray data

X-ray oriented powder patterns of chlorite concentrated from vein 2 show sharp basal reflections, with a mean d_{002} equal to 14.12 Å. From unoriented mounts, the following unit-cell parameters have been calculated: *a* 5.36, *b* 9.30, *c* 28.46 Å, β 97.23°. Chlorite samples from graywacke,

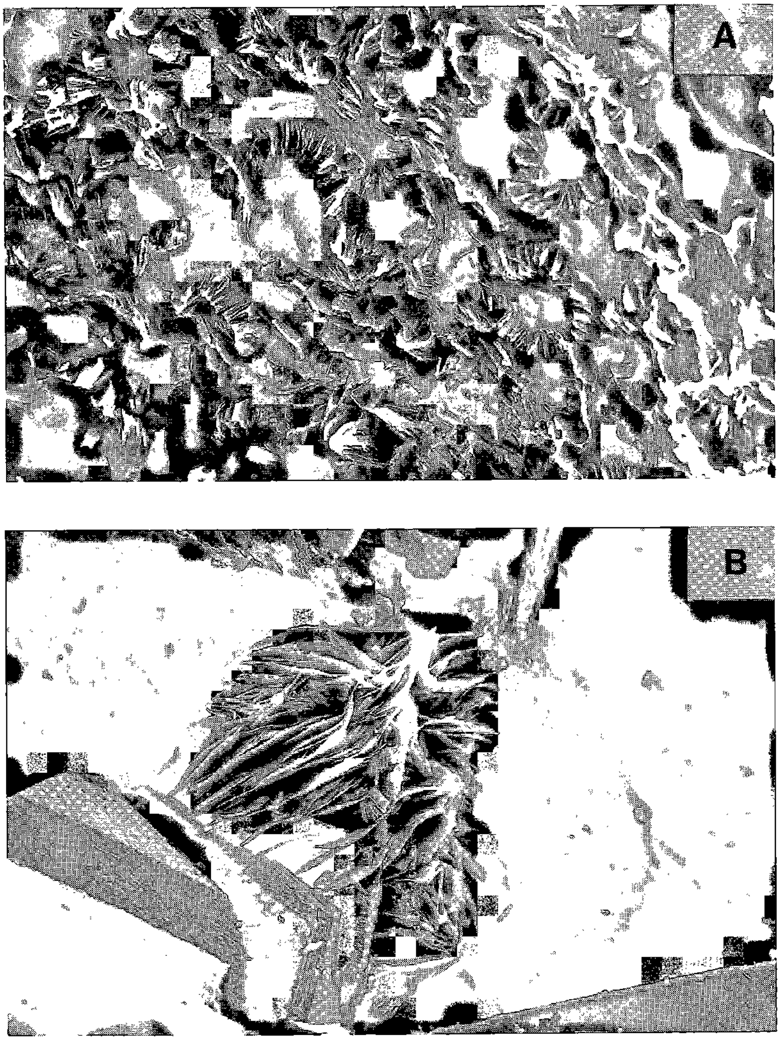

FIG. 3. SEM photomicrographs of chlorite and quartz filling veins. A. Vermicular chlorite from vein 2. B. Chlorite from thin veins showing large curved plates and, between these, some stacks of nacrite. Vein 1.

shale and phyllite samples show similar patterns, although the presence of mica obstructs the accurate determination of cell parameters.

The differences in the Fe content do not greatly affect the ratio of basal intensities, and hence I_{001}/I_{002} ranges from 0.25 to 0.33 in the analyzed samples. The ratio I_{003}/I_{001} has been used to determine the distribution of the octahedrally coordinated Fe between the 2:1 layer and the interlayer hydroxide sheet (Brown & Brindley 1980). This ratio ranges from 1.0 in chlorite from graywacke, shale and phyllite to 1.2–2.0 in chlorite from veins. From these values, the degree of asymmetry (D) or number of Fe atoms in the 2:1 layer minus number of Fe atoms in the interlayer sheet, has been calculated. D values range from –0.12 (almost symmetrical distribution), in chlorite from graywacke, shale and phyllite, to –0.56 in chlorite from veins, where Fe preferentially occupies the interlayer hydroxide sheet.

Infrared data

Variations in the infrared (IR) spectra of the chlorite samples studied depend on the chlorite content (Fig. 6). In the IR spectrum of chlorite from vein 2 (Fig. 6A), the position and relative intensity of the two bands associated with the interlayer hydroxyl groups agree with the

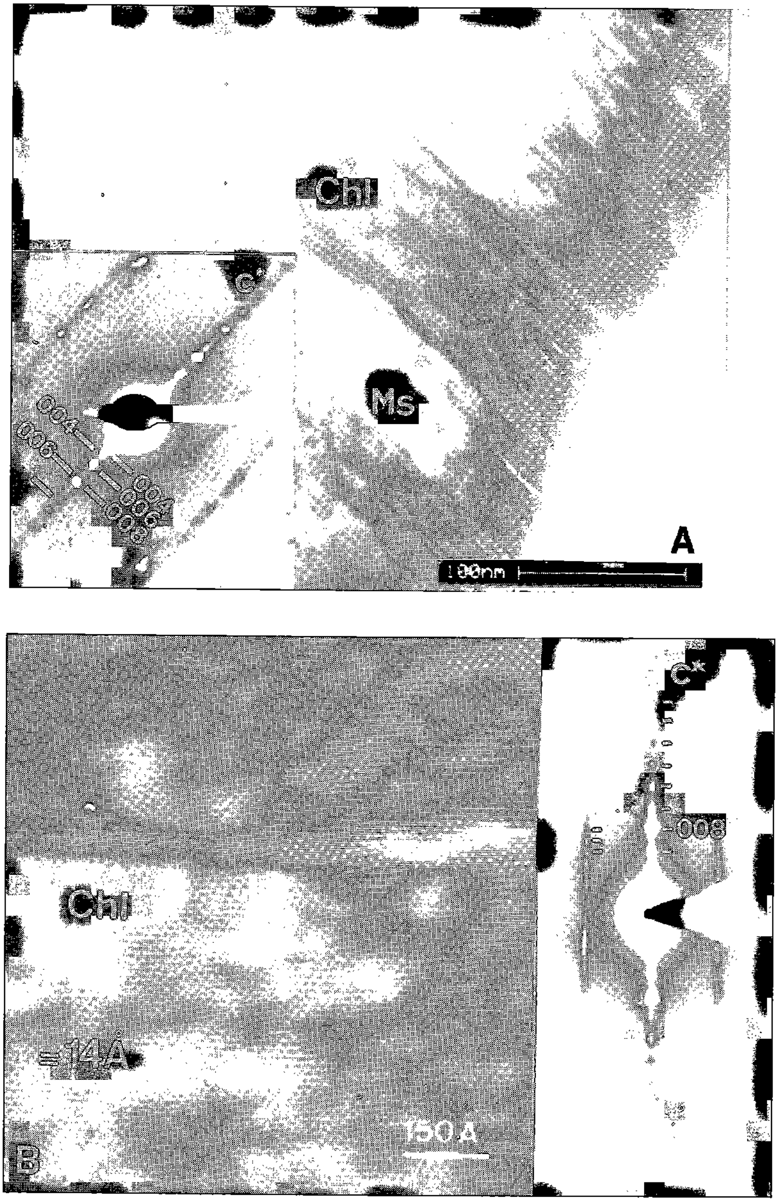

FIG. 4. A. TEM images of chlorite–mica stacks from sample 4, showing chlorite (Chl) and muscovite (Ms) packets. Insert: Corresponding SAED pattern displaying superimposed chlorite and muscovite 00*l* reflections, and ill-defined non-basal reflections. B. Lattice-fringe image of chlorite from vein 2, showing regular 14 Å periodicity. Insert: SAED pattern of chlorite, displaying 00*l* and 0*kl* reflections. Chlorite and muscovite indexing is based on a two-layer polytype.

spectra compiled by Farmer (1974) for Mg-rich and Fe-rich chlorite with similar Al contents. Spectra B and C (Fig. 6) belong to < 2 μm size fractions of samples 2 and 6, with different chlorite:mica ratios. Sample 2 shows the absorption band of the mica at 3628 cm^{-1}, and a single wide band at 3444 cm^{-1}, ascribed to chlorite. Sample 6 shows, in addition to the mica bands (at 3705 and 3628 cm^{-1}), three bands, at 3561, 3475 and 3427 cm^{-1}, the spectrum being similar to that characteristic of di,trioctahedral chlorites (Farmer 1974).

TABLE 3. RESULTS OF ELECTRON-MICROPROBE ANALYSES OF CHLORITE (wt%)

	Sample 1								Sample 3			Sample 5				Vein 1		Vein 3	
	A (4)	σ	B (3)	σ	C (4)	σ	D (44)	σ	A (4)	σ	B (1)	A (3)	σ	C (3)	σ	(8)	σ	(5)	σ
SiO_2	25.32	1.01	25.11	0.66	25.15	1.10	24.57	0.44	25.36	0.83	26.64	27.47	0.70	25.73	0.50	29.38	0.94	25.75	0.17
Al_2O_3	20.33	0.67	21.30	0.52	22.70	0.88	21.48	0.24	21.63	0.33	22.67	19.27	0.86	22.84	0.42	21.47	1.13	23.30	0.28
FeO	31.35	2.31	29.86	1.40	24.66	1.15	34.62	1.37	27.34	2.80	17.95	29.98	1.03	28.83	1.73	13.25	1.53	23.70	0.93
MgO	10.16	1.28	10.52	0.98	11.19	0.30	7.33	0.73	12.51	3.00	18.24	10.13	1.20	9.76	0.98	21.40	0.64	15.07	0.70
MnO	0.38	0.10	0.18	0.08	0.27	0.15	0.08	0.10	0.30	0.10	0.67	0.06	0.38	–	–	0.06	0.03	0.35	0.29
TiO_2	0.04	0.01	0.06	0.02	0.06	0.02	–	–	0.07	0.08	0.03	1.09	0.10	0.03	0.01	0.03	0.01	0.02	0.03
K_2O	0.06	0.02	0.17	0.08	0.02	0.01	0.02	0.01	0.01	0.02	0.03	0.11	0.10	0.25	0.12	0.15	0.10	0.05	0.03
Na_2O	--	–	0.04	0.08	0.03	0.02	–	–	0.01	0.01	0.06	0.06	0.08	0.08	0.10	0.06	0.02	0.05	0.02
CaO	0.02	0.01	0.01	0.01	–	--	0.01	–	0.02	0.02	0.03	0.05	0.02	0.02	0.02	0.03	0.01	0.02	0.00
Total	87.66	0.31	88.24	0.28	84.08	0.71	88.10	0.42	87.23	0.30	86.35	88.21	0.41	87.46	0.36	85.77	0.57	88.31	0.43
Si	2.76		2.73		2.75		2.71		2.70		2.74	2.92		2.76		2.91		2.69	
^{IV}Al	1.24		1.27		1.25		1.29		1.30		1.26	1.08		1.24		1.09		1.31	
^{VI}Al	1.38		1.45		1.66		1.51		1.43		1.48	1.37		1.63		1.50		1.54	
Fe	2.85		2.70		2.24		3.18		2.45		1.55	2.68		2.57		1.10		1.97	
Mg	1.64		1.70		1.83		1.21		1.99		2.79	1.61		1.56		3.23		2.33	
Mn	0.03		0.02		0.03		0.02		0.03		0.06	–		–		0.01		0.04	
Ti	–		–		--		–		0.01		–	0.09		–		–		–	
K	0.01		0.03		0.02		–		–		–	0.02		0.03		0.02		–	
Na	–		0.01		0.01		–		–		0.01	0.01		0.02		0.01		0.01	
Ca	–		--		0.03		–		–		–	–		–		–		–	
Total oct.	5.90		5.87		5.76		5.92		5.91		5.81	5.66		5.76		5.84		5.89	
Fe/(Fe+Mg)	0.63		0.61		0.61		0.72		0.55		0.36	0.62		0.62		0.25		0.45	
δAl	0.14		0.18		0.41		0.22		0.13		0.22	0.31		0.39		0.41		0.23	

A: Oxidized chlorite. B: Chlorite after biotite. C: Chlorite from chlorite-mica stacks. D: Interstitial chlorite. (n°): number of analyses
Formulae have been calculated on the basis of 14 oxygen equivalents.

DTA–TG data

DTA and TG curves of chlorite from veins are characterized by a large endothermic peak at 580–600°C, followed by a small exothermic effect at 816°C. This curve is clearly different from those of trioctahedral chlorites, which yield curves where the large endothermic peak occurs between 600 and 650°C and a clear endothermic–exothermic system appears at 800–900°C. The curves are consistent with di- or di,trioctahedral minerals, in which the recrystallization of new phases does not occur immediately upon dehydroxylation, as in trioctahedral minerals (Mackenzie 1970). TG curves reveal that the complete loss in mass occurs in the range 550–730°C. Thus, both the interlayer and the inner OH groups are lost in a narrow temperature-interval, and this explains the lack of high-temperature endo-exothermic effects.

DISCUSSION

Although some ferric iron is present in these chlorites, the formulae calculated assuming all iron to be ferrous have been used in the following figures and discussion, in order to facilitate the comparison with most of the diagenetic and very low-grade chlorites, characterized by electron microprobe (*e.g.* Curtis *et al.* 1985, Hillier & Velde 1991).

A plot of the analyzed samples of chlorite on the diagram proposed by Hey (1954) permits the distinction of the several types of chlorite (Fig. 7) on the basis of the Fe/(Fe + Mg) value. On this plot, chlorite from Alpine-type veins and segregations shows the largest variation. Most of the analyzed material plots below the line of birefringence = 0 (a), that is to say, in the zone of positive optic sign. Nevertheless, except for chlorite samples from veins 1 and 3, which show a variable optic sign, the chlorite has a negative optic sign. The compositional variation in chlorite from these veins permits the drawing of the line of birefringence = 0 (b) for the suite of chlorite samples from Maláguide. The slope and position of this line explain the simultaneous increase of refringence and birefringence in this material.

Shau *et al.* (1990) interpreted the anomalous optic sign of chlorite on the basis of changes in polarizability induced by the mixed-layering of smectite-like or vermiculite-like layers in chlorite, and they suggested that it is most probably the cause of optic anomalies in low-grade chlorite from other localities. In our case, X-ray patterns, chemical data and high-resolution images indicate that these types of interstratifications, common in the Maláguide Complex (Ruiz Cruz 1995), are absent in the analyzed samples. Therefore, it is more likely that the anomalous optics are related to the presence of Fe^{3+}.

Deer *et al.* (1962) stated that some samples of Fe-rich chlorite yield formulae with incomplete occupancy of octahedra if total Fe is expressed as FeO. These types of chlorite show considerable replacement of Al by Fe^{3+}, as in di,trioctahedral chlorites. A large proportion of these samples contain in excess of 4 wt.% Fe_2O_3 and were termed oxidized chlorite. This type of chlorite has $0 < 2V < 20°$ and a negative optic sign. According to the classification of Newman & Brown (1987), di,trioctahedral chlorites are Al-rich varieties (cookeite and sudoite), in which occupancy of octahedra ranges from 4.70 to 5.15 atoms per formula. The formulae of the chlorite samples from Maláguide (Table 3), calculated with total Fe expressed

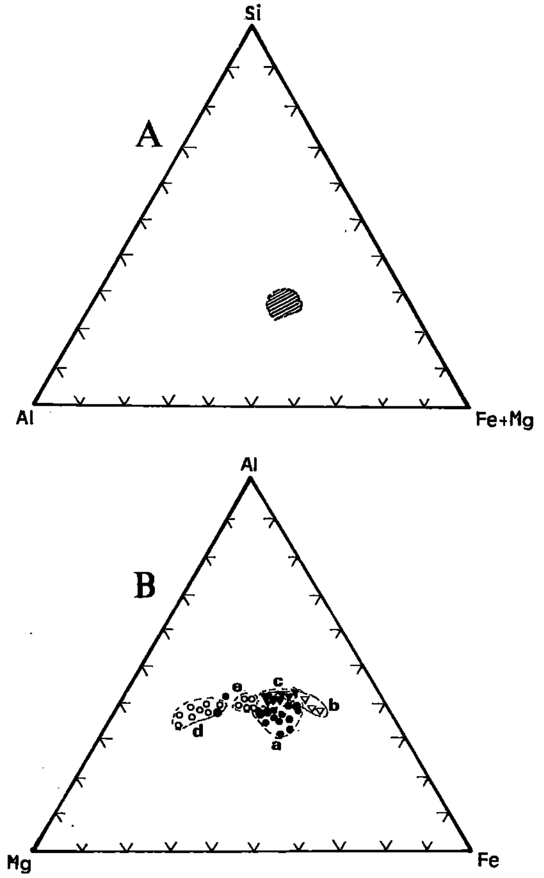

FIG. 5. A. In the Si – Al – (Fe + Mg) diagram, the analyzed specimens occupy a narrow zone (shaded). B. In the Al – Fe – Mg diagram, five zones can be separated: Zone a: chlorite after biotite and oxidized chlorite. Zone b: interstitial chlorite. Zone c: chlorite from chlorite–mica stacks. Zone d: chlorite from vein 3. Zone e: chlorite from vein 1. Small full circles: oxidized chlorite. Large full circles: chlorite after biotite. Open circles: chlorite from veins. Full triangles: chlorite from chlorite–mica stacks. Open triangles: interstitial chlorite.

as FeO, lead to occupancies between 5.55 and 5.99 in the octahedral site, clearly within the range defined by Newman & Brown for trioctahedral chlorites (5.50–5.99). Nevertheless, the H_2O content of the analyzed material is in many cases greater than 13%, and chemical analyses of quartz–chlorite veins and segregations (Table 5) confirm the presence of about 4 wt.% Fe_2O_3. If one assumes similar Fe^{2+}/Fe^{3+} values for all chlorites, the calculated formulae show $^{IV}Al/^{VI}Al$ ratios near 1, and the occupancy of octahedra decreases to 5.10–5.65, near the values of di,trioctahedral chlorite.

TABLE 4. RESULTS OF ATEM ANALYSES OF CHLORITE

	Sample 4		Sample 8		Vein 2		Segregation	
	C (5)	σ	A (6)	σ	(10)	σ	(8)	σ
Si *apfu*	2.68	0.15	2.73	0.06	2.66	0.08	2.74	0.16
^{IV}Al	1.32	0.15	1.27	0.06	1.34	0.08	1.26	0.16
^{VI}Al	1.45	0.08	1.40	0.03	1.59	0.12	1.37	0.20
Fe	2.88	0.25	2.29	0.12	2.49	0.23	2.29	0.42
Mg	1.57	0.16	2.20	0.05	1.62	0.10	2.18	0.35
Mn	0.01	0.01	0.02	0.01	0.01	0.01	0.02	0.01
Na	–		0.02	0.02	–		–	
K	–		0.01	–	–		0.02	0.01
Ca	–		0.01	–	0.06	0.01	0.07	0.02
Total oct.	5.91	0.07	5.91	0.03	5.71	0.09	5.86	0.05
Fe/(Fe + Mg)	0.65	0.03	0.51	0.03	0.61	0.03	0.51	0.12
δAl	0.13	0.06	0.13	0.04	0.25	0.11	0.11	0.08

A: Oxidized chlorite, C: Chlorite from stacks. In parentheses, number of analyses.

Figure 8 shows the compositional trend in different generations of chlorite, represented on the diagram of Curtis *et al.* (1985). Oxidized chlorite and that developed from biotite, except for two cases, fall near the lower boundary of the enclosure defined by these authors for metamorphic chlorite, to a great extent within the chamosite field. The range of ^{IV}Al content is narrow, and the fields of chlorite samples from the lower to the upper Paleozoic overlap (Fig. 8A). This fact points to a similar origin for both types of chlorite, also suspected from textural relations. A similar position in the diagram is occupied by the chlorite from chlorite–mica stacks, which developed during the same metamorphic event, but probably from different precursor phases. Interstitial authigenic chlorite plots in the more Fe-rich part of the diagram. Chlorite from the thick veins, probably developed during this metamorphic event, also plots in the chamosite field, and shows the highest ^{IV}Al content. In this manner, prograde Variscan metamorphism seems to be characterized by a slight increase of Fe content and, probably, ^{IV}Al content. The chlorite from veins and segregations structurally related to the Alpine deformations (Fig. 8B) occupies a large area from the clinochlore to the chamosite field. Chlorite from vein 1 occupies a zone that appears unoccupied in the plot of Curtis *et al.* (1985), whereas chlorite from the structurally deepest samples plots near the boundary clinochlore–chamosite. These chlorite samples show a wide variation in ^{IV}Al content, indicating that prograde Alpine metamorphism is reflected

TABLE 5. RESULTS OF WET-CHEMICAL ANALYSES OF QUARTZ–CHLORITE VEIN AND SEGREGATION

	SiO_2	Al_2O_3	Fe_2O_3	FeO	MgO	MnO	CaO	K_2O	Na_2O	TiO_2	P_2O_5	Total
Vein 2 wt%	68.47	7.47	2.34	7.74	3.07	0.20	3.04	0.08	0.08	0.06	0.05	92.58
Segregation	62.99	9.25	3.01	10.07	7.34	0.08	0.51	0.03	0.01	0.02	0.08	93.30

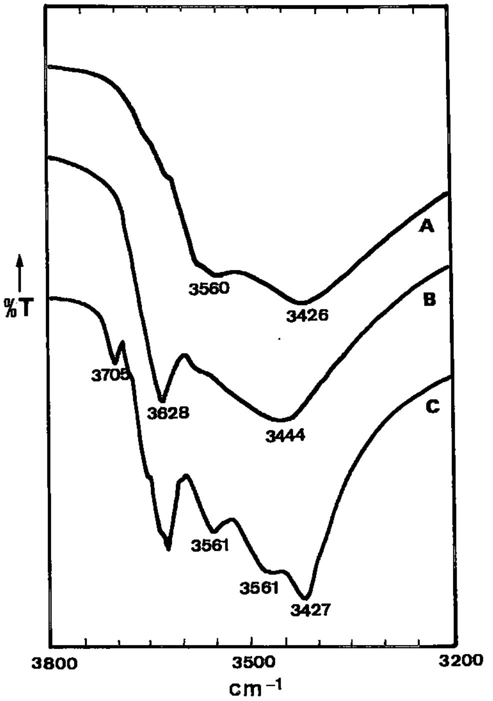

FIG. 6. IR spectra of chlorite-rich samples. A. Chlorite from vein 2. B. <2 µm size fraction of sample 2, containing 26% Chl, 74% Ms. C. <2 µm size fraction of sample 6, containing 45% Chl, 55% Ms.

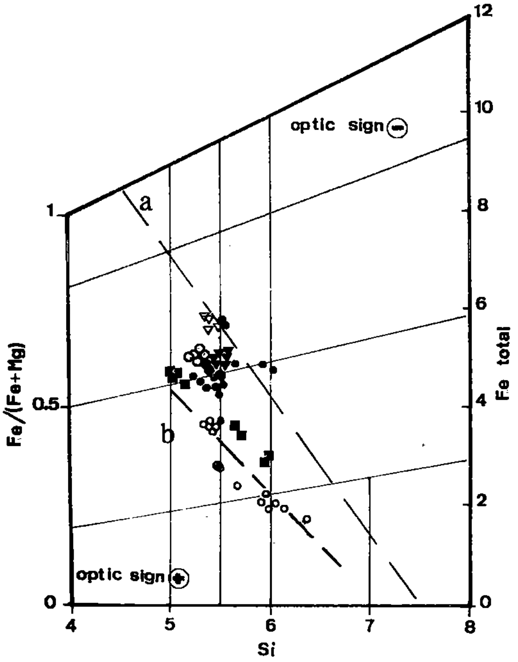

FIG. 7. Plot of the analyzed samples on the diagram by Hey (1954). Line (a) corresponds to birefringence = 0, as deduced for normal chlorite. Line (b) corresponds to birefringence = 0 for chlorite from the Maláguide Complex. Small full circles: oxidized chlorite. Large full circles: chlorite after biotite. Full triangles: chlorite from chlorite–mica stacks. Open triangles: interstitial chlorite. Small open circles: chlorite from veins 1 and 3. Large open circles: chlorite from vein 2. Squares: chlorite from segregation.

in a simultaneous increase in ^{IV}Al and Fe/(Fe + Mg). This trend of increasing ^{IV}Al and Fe/(Fe + Mg) contents with increasing metamorphism has been described previously (*e.g.*, Shirozu 1978, Bailey 1988).

The proportion of ^{IV}Al depends on the temperature of formation of chlorite and has been used as geothermometer (Cathelineau & Nieva 1985, Kranidiotis & MacLean 1987, Cathelineau 1988). Nevertheless, from the results of De Caritat *et al.* (1993), it seems clear that none of the available geothermometers satisfactorily predicts the temperature of formation of chlorite. Nevertheless, whatever the relation used, the ^{IV}Al content is undoubtedly linked to the temperature evolution within a homogeneous geochemical medium (De Caritat *et al.* 1993). Ruiz Cruz & Andreo (1996) used the relation proposed by Hillier & Velde (1991), deduced from diagenetic and very low-grade chlorite, and estimated temperatures of about 150°C for Permo-Triassic material, and about 280°C for Paleozoic material in the Málaga area. This discontinuity was interpreted as evidence for a metamorphic event older than Alpine metamorphism. The new data summarized here establish the metamorphic conditions in which the chlorite populations have developed. Since the relation deduced by Hillier & Velde (1991), as well as most of the empirical calibrations relating ^{IV}Al and temperature, are based on results of electron-microprobe analyses, temperatures of formation have been calculated from the ^{IV}Al values determined assuming all Fe as Fe^{2+}. These temperatures can be considered as minimal values, since the presence of Fe^{3+} would lead to an increase of ^{IV}Al in the calculated formulae. The textural data indicate that oxidized chlorite and that developed from the alteration of biotite are clearly related to Variscan metamorphism. These chlorites show uniform ^{IV}Al contents throughout the Paleozoic sequence, and yield temperatures in the order of 300°C for most of these samples. Similar temperatures are deduced from the interstitial chlorite, whereas chlorite from chlorite–mica stacks and chlorite from vein 2 yield slightly higher temperatures. The uniformity in chemical composition seems to indicate that these samples of chlorite equilibrated during Variscan metamorphism. In contrast, temperatures calculated from the Alpine veins and segregations range from 150°C to >300°C, and show a clear relationship to stratigraphic position. In this manner, the conditions of Alpine metamorphism uniformly increased from Permo-Triassic to Paleozoic materials, as is also manifested by the evolution of kaolinite-type minerals (Ruiz Cruz 1996) and illite crystallinity (IC) values (Fig. 9).

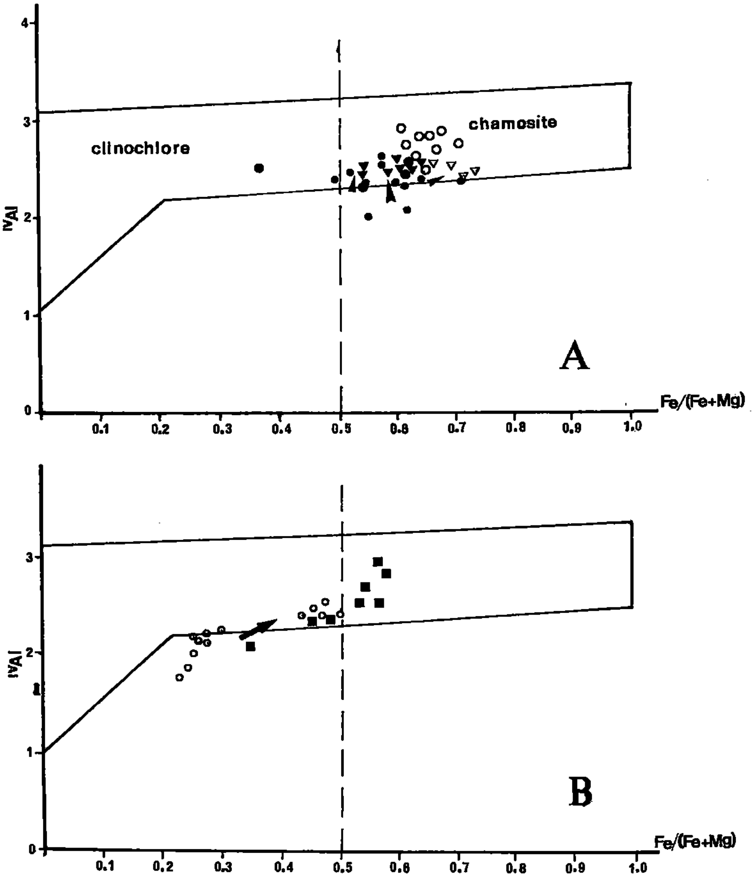

FIG. 8. Plot of the analyzed samples on the diagram of Curtis *et al.* (1985). A. Chlorite ascribed to Variscan metamorphic event. B. Chlorite ascribed to Alpine metamorphic event. Arrows indicate the chemical trends in progressive metamorphism. Small full circles: oxidized chlorite. Large full circles: chlorite after biotite. Full triangles: chlorite from chlorite–mica stacks. Open triangles: interstitial chlorite. Small open circles: chlorite from veins 1 and 3. Large open circles: chlorite from vein 2. Squares: chlorite from segregation.

These results indicate that the Alpine metamorphism was characterized in a majority of the Malâguide samples by temperatures lower than those attained during the Variscan episode of metamorphism, leading to a preservation of the chemical features of Variscan chlorite.

CONCLUSIONS

1. The chlorite found throughout the Malâguide Complex has abnormal optical properties and low $^{IV}Al/^{VI}Al$ values if all Fe is assumed as Fe^{2+}. Nevertheless, in contrast to other cases of anomalous low-grade chlorite, XRD patterns, M^+ contents, and TEM images indicate the absence of mixed layering with smectite- or vermiculite-type minerals.

2. The H_2O content in the analyzed samples of chlorite, as well as the proportion of ferrous iron, indicate that a part of the Fe content (about one quarter of the total Fe) is Fe^{3+}. These values yield more accurate formulae, and occupancies of the octahedral position between 5.10 and 5.65 *apfu*, near the values accepted for di,trioctahedral chlorites. Thermal behavior and some of the IR spectra seem to confirm the di,trioctahedral nature of these samples. Optical properties may also be correlated with total Fe content and with Fe^{3+} content.

3. Chlorite developed during the Variscan metamorphism shows a homogeneous composition throughout the Paleozoic sequence, whereas a simultaneous increase in ^{IV}Al and Fe/(Fe + Mg) characterizes the chlorite equilibrated during the low-temperature Alpine metamorphism.

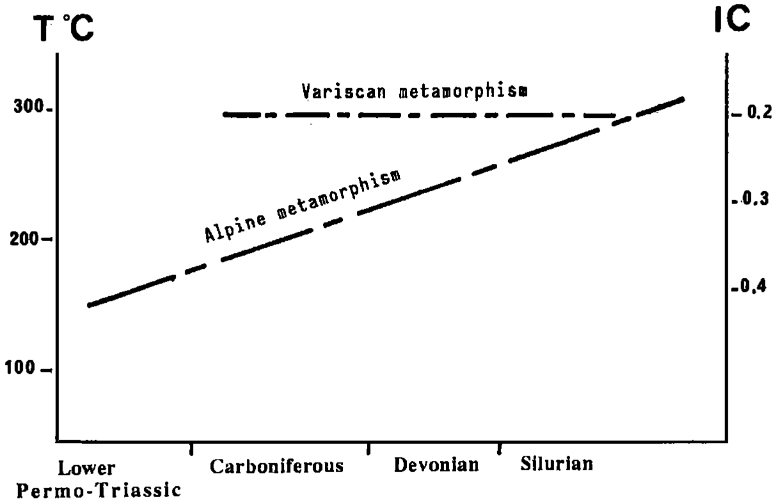

FIG. 9. Temperatures estimated for the Variscan and the Alpine metamorphic events, as a function of the depth, and mean values of the illite crystallinity (IC).

REFERENCES

ALBEE, A.L. (1962): Relationships between the mineral association, chemical composition and physical properties of the chlorite series. *Am. Mineral.* **47**, 851-870.

BAILEY, S.W. (1988): Chlorites: structures and crystal chemistry. *In* Hydrous Phyllosilicates (S.W. Bailey, ed.). *Rev. Mineral.* **19**, 347-403.

BAIN, C.D. & SMITH, B.F.L. (1992): Chemical analyses. *In* Clay Mineralogy: Spectroscopic and Chemical Determinative Methods (M.J. Wilson, ed.). Chapman & Hall, London, U.K. (300-332).

BEAUFORT, D. (1987): Interstratified chlorite/smectite ("metamorphic vermiculite") in the upper Precambrian greywackes of Rouez, southern France. *In* Proc. Int. Clay Conf. (Denver, 1985; L.G. Schultz, H. Van Olphen & F. A. Mumpton, eds.). The Clay Mineral Society, Bloomington, Indiana (59-65).

BROWN, G. & BRINDLEY, G.W. (1980): X-ray diffraction procedures for clay mineral identification. *In* Crystal Structures of Clay Minerals and their X-ray Identification (G.W. Brindley & G. Brown, eds.). Mineral. Society, London, U.K. (305-360).

CATHELINEAU, M. (1988): Cation site occupancy in chlorites and illites as a function of temperature. *Clay Mineral.* **23**, 471-485.

________ & NIEVA, D. (1985): A chlorite solid solution geothermometer. The Los Azufres geothermal system (Mexico). *Contrib. Mineral. Petrol.* **91**, 235-244.

CRAW, D. & JAMIESON, R.A. (1984): Anomalous optics in low-grade chlorite from Atlantic Canada. *Can. Mineral.* **22**, 269-280.

CURTIS, C.D., HUGHES, C.R., WHITEMAN, J.A. & WHITTLE, C.K. (1985): Compositional variation within some sedimentary chlorites and some comments on their origin. *Mineral. Mag.* **49**, 375-386.

DEER, W.A., HOWIE, R.A. & ZUSSMAN, J. (1962): *Rock-Forming Minerals.* **3**. *Sheet Silicates.* J. Wiley & Sons, New York, N.Y.

DE CARITAT, P., HUTCHEON, I. & WALSHE, J.L. (1993): Chlorite geothermometry: a review. *Clays Clay Minerals* **41**, 219-239.

DÍAZ DE FEDERICO, A., TORRES ROLDÁN, R. & PUGA, E. (1990): The rock series of the Betic substratum. *In* Le Bassin Néogène du Domaine Bétique Oriental. *Document et Travaux, IGAL* (Paris), 12-13, 19-29.

FARMER, V.C. (1974): The layer silicates. *In* The Infrared Spectra of Minerals (V.C. Farmer ed.). Mineral. Society, London, U.K. (331-363).

FONTBOTÉ, J.M. & VERA, J.A. (1984): La Cordillera Bética. *In* Geología de España. *Inst. Geol. Mineral. Esp.* **2**, 205-343.

FREY, M. (1987): Very low-grade metamorphism of clastic sedimentary rocks. *In* Low Temperature Metamorphism (M. Frey, ed.). Blackie, Glasgow, U.K. (9-226).

GARCÍA LÓPEZ, S., RODRÍGUEZ CAÑERO, R., SANZ-LÓPEZ, J., SARMIENTO, G. & VALENZUELA-RIOS, J.I. (1996): Conodontos y episodios carbonáticos en el Silúrico de la cadena herciniana meridional y del dominio Sahariano. *Rev. Esp. Paleont.* (in press).

HEY, M.H. (1954): A new review of the chlorites. *Mineral. Mag.* **30**, 277-292.

HILLIER, S. & VELDE, B. (1991): Octahedral occupancy and the chemical composition of diagenetic (low-temperature) chlorites. *Clay Mineral.* **26**, 149-168.

JIAN, W.-T. & PEACOR, D.R. (1994): Formation of corrensite, chlorite and chlorite-mica stacks by replacement of detrital biotite in low grade pelitic rocks. *J. Metamorphic Geol.* **12**, 867-884.

KRANIDIOTIS, P. & MACLEAN, W.H. (1987): Systematic of chlorite alteration at the Phelps Dodge massive sulfide deposit, Matagami, Quebec. *Econ. Geol.* **82**, 1898-1911.

LAIRD, J. (1988): Chlorites: metamorphic petrology. *In* Hydrous Phyllosilicates (S.W. Bailey, ed.). *Rev. Mineral.* **19**, 405-453.

MACKENZIE, R.C. (1970): Simple phyllosilicates based on gibbsite- and brucite-like sheets. *In* Differential Thermal Analysis (R.C. Mackenzie, ed.). Academic Press, London, U.K. (498-537).

MÄKEL, G.G. (1985): The geology of the Malaguide Complex and its bearing on the geodynamic evolution of the Betic-Rif orogen (southern Spain and northern Marocco). *Gua Papers of Geology* **22**, 263 pp.

MORAD, S. & ALDAHAN, A.A. (1986): Diagenetic alteration of detrital biotite in Proterozoic sedimentary rocks from Sweden. *Sed. Geol.* **47**, 95-107.

NEWMAN, A.C.D. & BROWN, G. (1987): The chemical constitution of clays. *In* Chemistry of Clays and Clay Minerals (A.C.D. Newman, ed.). *Mineralogical Society, Monogr.* **6**, 1-128.

RUIZ CRUZ, M.D. (1995): Some mixed-layer minerals from very low-grade metamorphic origin (Betic Cordilleras, Spain). *8th Euroclay Conf.*, 333 (abstr.).

________ (1996): Nacrite, dickite and possible dickite/nacrite mixed-layers from the Betic Cordilleras (Spain). *Clays Clay Minerals* **44**, 357-369.

________ & ANDREO, B. (1996): Genesis and transformation of dickite in Permo-Triassic sediments (Betic Cordilleras, Spain). *Clay Mineral.* **31**, 133-152.

SAGGERSON, E.P. & TURNER, L.M. (1982): General comments on the identification of chlorite in thin section. *Mineral. Mag.* **46**, 469-473.

SHAU, Y.-H., PEACOR, D.R. & ESSENE, E.J. (1990): Corrensite and mixed-layer chlorite/corrensite in metabasalt from northern Taiwan: TEM/AEM, EMPA, XRD, and optical studies. *Contrib. Mineral. Petrol.* **105**, 123-142.

SHIROZU, H. (1978): Chlorite minerals. *In* Clays and Clay Minerals of Japan (T. Sudo & S. Shimoda, eds.). Elsevier, Amsterdam, The Netherlands (243-264).

VELDE, B. (1984): Electron microprobe analysis of clay minerals. *Clay Mineral.* **19**, 243-247.

________ (1985): *Clay Minerals: a Physico-Chemical Explanation of their Occurrence*. Elsevier, Amsterdam, The Netherlands.

WHITE, S.H., HUGGETT, J.M. & SHAW, H.F. (1985): Electron-optical studies of phyllosilicate intergrowths in sedimentary and metamorphic rocks. *Mineral. Mag.* **49**, 413-423.

Received August 6, 1995, revised manuscript accepted July 15, 1997.